

# Microglial Deletion and Inhibition Alleviate Behavior of Post-Traumatic Stress Disorder in Mice

**Shuoshuo Li**

Institute of Basic Medical Sciences <https://orcid.org/0000-0003-3499-2717>

**Yajin Liao**

Minzu University of China

**Yuan Dong**

Qingdao University Medical College

**Xiaoheng Li**

School of Basic Medical Sciences

**Jun Li**

Capital Medical University

**Yong Cheng**

Minzu University of China

**Jinbo Cheng**

Minzu University of China

**Zengqiang Yuan** (✉ [zyuan620@yahoo.com](mailto:zyuan620@yahoo.com))

<https://orcid.org/0000-0001-5739-2867>

---

## Research

**Keywords:** Mass cytometry, Microglia, Microglial depletion, Microglial activation, PTSD

**Posted Date:** June 29th, 2020

**DOI:** <https://doi.org/10.21203/rs.3.rs-37471/v1>

**License:**   This work is licensed under a Creative Commons Attribution 4.0 International License.

[Read Full License](#)

---

**Version of Record:** A version of this preprint was published on January 5th, 2021. See the published version at <https://doi.org/10.1186/s12974-020-02069-9>.

# Abstract

**Background:** Alteration of immune status in the central nervous system (CNS) has been implicated in the development of Post-Traumatic Stress Disorder (PTSD). However, the nature of overall changes in brain immunocyte landscape in PTSD condition remains unclear.

**Methods:** We constructed a mouse PTSD model by electric foot-shocks followed by contextual reminders and verified the PTSD-related symptoms by behavior test (including contextual freezing test, open field test and elevated plus maze test). We examined the immunocyte panorama in the brains of the naïve or PTSD mice by using single cell mass cytometry. Microglia number and morphological changes in hippocampus, prefrontal cortex and amygdala were analyzed by histopathological methods. The gene expression changes of those microglia were detected by quantitative real-time PCR. Genetic/pharmacological depletion of microglia or minocycline treatment before foot-shock exposure were performed to study the role of microglia in the PTSD development and progress.

**Results:** We found microglia are the major brain immune cells respond to PTSD. The number of microglia and ratio of microglia to immunocytes was significantly increased on the fifth day of foot-shock exposure. Furthermore, morphological analysis and gene expression profiling revealed temporal patterns of microglial activation in the hippocampus of PTSD brains. Importantly, we found that genetic/pharmacological depletion of microglia or minocycline treatment before foot-shock exposure alleviated PTSD-associated anxiety and contextual fear.

**Conclusion:** Our results demonstrated a critical role for microglial activation in PTSD development and a potential therapeutic strategy for the clinical treatment of PTSD in the form of microglial inhibition.

## Introduction

Post-traumatic stress disorder (PTSD) is a psychiatric disorder that develops after an individual is exposed to traumatic events. Although a commonly occurring disorder, the mechanisms underlying PTSD development still remain unclear. A growing body of evidence shows that imbalances in immune system and hyperactive neuroinflammatory responses may play a role in the development of PTSD<sup>1,2</sup>. In the peripheral immune system, PTSD patients have shown higher numbers of Th1 cells and impaired function of Treg cells<sup>3,4</sup>. Moreover, some pro-inflammatory cytokines including tumor necrosis factor  $\alpha$  (TNF $\alpha$ ), interleukin-6 (IL-6) and interleukin-1 $\beta$  (IL-1 $\beta$ ) were also significantly increased in the serum of PTSD patients<sup>5,6</sup>. Therefore, neuroinflammation might be a significant contributor to PTSD pathology.

Microglia constitute the major type of immune cells in the central nervous system (CNS) and are involved not only in the development of Alzheimer's disease<sup>7</sup>, Parkinson's disease<sup>8</sup> and stroke<sup>9</sup>, but also in depression by regulating synaptic function<sup>10</sup>. Recently, RNA sequencing results from PTSD model mice showed differential expression patterns of cytokines in various areas of the brain<sup>11</sup>. Microglia-derived pro-inflammatory cytokines are correlated with affective behaviors<sup>12</sup> and an endotoxin challenge has

been shown to activate microglia, leading to negative emotional disorders<sup>12,13</sup>. In keeping with these findings, inhibiting cytokine production can also alleviate depression-like symptoms<sup>14</sup>. Interestingly, antidepressant drugs targeting 5-hydroxytryptamine (5-HT) can suppress depression-induced microglial activation<sup>15</sup>. Together, these evidences strongly suggest that microglia are involved in the development of PTSD.

Microglial activation is always accompanied by dynamic changes in morphology and polarization<sup>16,17</sup>. Pathological stimulation can induce morphological alterations of microglia such as extension/retraction of branch processes and changes in soma volume. Although the morphology and expression patterns of immunoregulatory proteins in microglia vary among different brain areas under normal physiological conditions, the morphological alterations seen in injured brains are region-specific<sup>18,19</sup>. It has been shown that the number of microglia dynamically change in a depression model induced by chronic unpredicted stresses<sup>20</sup> and that chronic stress can cause structural reorganization of microglial morphology in the prefrontal cortex<sup>21</sup>. However, it is still largely unknown how the microglial status changes in different brain areas. The relationship between the morphology and microglial status under pathological conditions, especially in psychiatric disorders, also remains unclear. The prefrontal cortex (PFC), hippocampus (HP) and amygdala (AMY) have been identified as the major brain areas involved in fear emotion regulation<sup>22-24</sup>, and fMRI studies indicate that activity alterations in these regions are involved in the development of PTSD<sup>25,26</sup>. Therefore, it would be of value to decipher the microglial alterations in these emotion-related brain areas during PTSD development.

Mass cytometry, also known as CyTOF (Cytometry by Time-Of-Flight), is a powerful flow cytometry technique developed in recent years. Similar to regular flow cytometry, mass cytometry can determine protein expression at a single cell level. However, the advantage of mass cytometry is its supreme sensitivity, achieved by using stable and unique heavy metal isotope-labeled antibodies to recognize cellular markers and analyzing them with a time-of-flight mass spectrometer. Using this technique, the immune cells of the murine CNS have been characterized with high dimensional resolution<sup>27</sup>, allowing the description of immune landscapes of the murine brain in steady state<sup>28</sup>, aging and neurodegeneration disease<sup>29</sup> and neuroinflammatory disease<sup>30</sup>. Therefore, CyTOF would be a useful tool to characterize the distribution of immune cells during the development of psychiatric disorders such as PTSD.

In this study, we utilized CyTOF to characterize the immunocytes in PTSD model brains and found that microglia constitute the majority of brain immunocytes in response to chronic stress. We further defined the features of microglia, including number, morphology and gene expression, in the different brain regions during PTSD development. We found significant correlations among the changes in microglial morphology, gene expression levels of proinflammatory cytokines and behavioral performance. Importantly, we examined the effect of genetic/pharmacological deletion of microglia or minocycline-mediated microglial suppression on the microglial morphology, gene expression and behavior in PTSD

model mice. Based on our findings, we argue that microglial inhibition offers a therapeutic avenue for PTSD treatment.

## Materials And Methods

### Animal housing

All mice used in this study were housed at room temperature, in a 12 h dark/light cycle (8:00 a.m. - 8:00 p.m.). Mice had free access to standard rodent chow and water. In order to avoid differences arising due to age and gender, only 2-4 month old male mice were used in this study. Mice in same group were housed together, with 3-4 mice in each cage. *Cx3cr1-GFP* mice were used as heterozygous mice. *Cx3cr1<sup>creER</sup>* and *iDTR* mice<sup>31</sup> were purchased from Jackson Laboratory. *Cx3cr1-GFP* mice were a kind gift from Dr. Junwei Hao of Tianjin Medical University.

All animal experiments were approved by the Institutional Animal Care and Use Committee at the Beijing Institute of Basic Medical Sciences (Beijing, China).

### Chemical administration

Sertraline (Cat. S6319, Sigma-Aldrich, Germany) was administered by intragastric gavage (i.g.) at a concentration of 15 mg/kg. Tamoxifen (TAM; Cat. S1238, Selleck, USA) was dissolved in sunflower beads oil containing 5% ethanol. 10 mg tamoxifen administered once a day for three consecutive days. For microglia depletion, 1 µg diphtheria toxin (DT; Cat. D0564, Sigma-Aldrich, Germany) injected intraperitoneally 3 weeks after TAM administration, once a day for three consecutive days. PLX3397 (Cat. S7818, Selleck, USA) was added to the diet at a concentration of 290 mg/kg and fed to the mice 21 days before delivering foot-shocks. Minocycline (Cat. S4226, Selleck, USA) was administered intragastrically at 40 mg/kg/day, 3 days before delivering foot-shocks. Sertraline, PLX3397, Minocycline were continually administered until all the behavior tests were completed.

### Behavior tests

All behavior tests were started at 10:00 a.m. and finished before 5:00 p.m. Each group contained eight or more mice and their littermates were used as control groups.

### Open field test

Open field test was conducted inside a clear box (50 cm x 50 cm x 20 cm). Activity was automatically monitored by ANY-maze software (Global Biotech, USA). The apparatus was washed with a 75% ethanol solution before each mouse was introduced. Each mouse was recorded for 5 mins and total distance, average speed, time spent and distance travelled in center area (25 cm x 25 cm) were the parameters that were analyzed.

### Elevated plus maze (EPM) test

The maze consisted of two open arms (35 cm × 5 cm) and two enclosed arms (35 cm × 5 cm × 15 cm) connected to a common central platform (5 cm × 5 cm). The apparatus was raised to a height of 50 cm from the floor and was lit by a dim light placed above the central platform. The maze was washed with a 75 % ethanol solution before each mouse was introduced. Time spent and distance traveled in open arms versus close arms was measured for a period of 5 min.

### **Electric foot-shock procedures**

The procedure for electric foot-shock was adapted from Zhang et al.<sup>32</sup> and Qiu et al.<sup>33</sup>. Electric foot-shocks were carried out in a fear-conditioning chamber (35 cm × 20 cm × 20 cm) (Jiliang Tech, China). After a 5 min adaptation period, 15 intermittent, inescapable foot-shocks were delivered to the mice (intensity: 0.8 mA; interval: 10 s; duration: 10 s). The control group mice were placed in the same chambers without stimulation for a total of 10 min to adapt to the same circumstance. Repeat stimulation on the second day enhances fear memory and increases the chances of developing PTSD. A 75% ethanol solution was used to wipe the chamber before each mouse was introduced, to avoid any effects of feces and odor.

### **Contextual freezing measurement**

In the fear contextual test, mice who have previously experienced foot-shocks will freeze intermittently when exposed to the chamber where the foot-shocks were delivered. This freezing behavior is associated with context-induced fear memory<sup>34</sup>. All mice were tested three times at different time points, with each test lasting for 5 min. The total cumulative freezing time and percentage of time spent frozen were recorded and analyzed by DigBehv software (Jiliang Tech, China).

### **Immunohistochemistry And immunofluorescence**

Immunohistochemistry was performed as previously described<sup>8</sup>. In brief, mouse brains were fixed with 4% paraformaldehyde after perfusion with saline. Fixed brains were dehydrated in 30% sucrose (in PBS). 20 mm thick coronal sections were cut throughout the whole brain and the sections were washed with PBS and incubated with 3% hydrogen peroxide (H<sub>2</sub>O<sub>2</sub>) for 15 min to inhibit endogenous peroxidases. After three washes with PBS, the sections were blocked for 1.5 hours with blocking buffer (0.3% Triton X-100 + 10% goat serum in PBS) at room temperature, followed by incubating with rabbit monoclonal anti-IBA1 (1:600; Cat. 019-19741, WAKO, Japan) and then visualized with biotinylated goat anti-rabbit IgG (1:200, Vectastain ABC kit, Vector Laboratories, USA), followed by streptavidin-conjugated horseradish peroxidase (Vectastain ABC kit, Vector Laboratories, USA) staining. The primary and secondary antibodies were diluted in blocking buffer. For immunohistochemistry, positive immunostaining was visualized with 3,30-diaminobenzidine (DAB kit, Zhongshanjinqiao, China). Stained sections were mounted onto slides and imaged using Nanozoomer (Hamamatsu, Japan). For immunofluorescence, Alexa Fluor 488-conjugated secondary antibody (1:400, Invitrogen, USA) was used. Nuclear morphology was visualized using Hoechst 33258 (Sigma, USA). *Cx3cr1-GFP* mice were stained only with the Hoechst. Immunofluorescence was imaged using a Nikon A1 confocal microscope (Nikon, USA).

## Image analysis

Images were captured using Nanozoomer (Hamamatsu, Japan) and Nikon A1 confocal microscope (Nikon, USA). The number of microglia and their soma area were automatically measured at 20x magnification for a defined area by Image Pro Plus (Media Cybernetics, Inc)(export image—count and measure objects—select color—count—view measurement data). For precision, we counted 2-3 fields of the targeted brain area for each slice, 5 consecutive slices from each mouse were analyzed and the average microglial density was calculated.

The skeleton analysis was done using ImageJ software (National Institutes of Health, USA). The images prepared for skeleton analysis were captured as a Z-series stack (20 mm) using Nikon A1 confocal microscope. Z-stack images were condensed into a maximum intensity projection image and converted to 8-bit using an ImageJ plugin and then skeletonized using the Skeletonize (2D/3D) plugin. Microglial process number and length were analyzed using the AnalyzeSkeleton plugin. The resulting parameters were used as measures of microglia morphology.

## Quantitative real-time PCR

The experiment was performed as previously described <sup>7</sup>. Briefly, total RNA was extracted from mouse brain tissue using TRIzol (Thermo Fisher, USA). Reverse transcription was performed using random primers. Quantitative PCR was performed using UltraSYBR supermix with ROX (CWBIO, China) and detected by ABI QuantStudio 3(Thermo Fisher, USA) apparatus. The housekeeping gene ACTB was used as an endogenous control. Gene expression levels were expressed as  $2^{-\Delta\Delta Ct}$ . Primer sequences for QPCR are listed in Supplementary Table 2.

## Tissue harvesting and single cell dissociation

After the first contextual fear response test (day 3), mice were sacrificed, their brains perfused with saline and the brain parenchyma harvested. Scissors were used to cut the brain parenchyma into small pieces, which were then digested for 30 min at 37° C in digestion buffer (PBS containing 2% FBS and 2 mg/ml collagenase  $\times$ ). The samples were homogenized with a syringe and filtered through a 70 mm cell strainer. After centrifugation at 600 g for 6 min, the acquired pellet was resuspended in 37% Percoll (GE Healthcare, USA) in PBS. This suspension was subjected to gradient centrifugation, with the gradients spanning 70% Percoll in PBS, 30% Percoll in PBS and only PBS (2000 g for 30 min at 4° C). The immunocytes were collected at the 37-70% interphase and washed once in PBS. The samples were then ready for staining with the mass cytometry antibody.

## Mass cytometry

The metal isotope-labeled antibodies used in mass cytometry were made using antibody-labeling kits from Fluidigm (Fluidigm, USA) and all the experiments were performed according to the manufacturer protocols. We first performed tests to ensure that all antibodies were effective and that the parameters

were informative. Five different anti-CD45 antibodies conjugated with Pd-104, Pd-105, Pd-106, Pd-108 and Pd-110 were used to label live cells<sup>35</sup>. Then, composite samples were incubated with a cocktail of primary antibodies. Barcoded composite samples were loaded onto a Helios mass cytometer (Fluidigm, USA) and the data were analyzed with MATLAB (MathWorks, China) and Cytobank software (Cytobank, USA). The results were present in viSNE map, heat map and Flow Self Organizing Map (FlowSOM).

## Statistical analysis

Statistical analyses were performed using ANOVA followed by Tukey's post hoc test or by a two-tailed Student's t-test, depending on the dataset. All values are expressed as mean  $\pm$  SEM. \*  $p < 0.05$ , \*\*  $p < 0.01$  and \*\*\*  $p < 0.001$  denote the significance thresholds.

# Results

## Microglia are the major brain immune cells respond to PTSD

We established a mouse model of post-traumatic stress disorder (PTSD) (**Figure S1A**) and found that two rounds of foot-shock significantly increased the contextual fear response on days 3, 8 and 15 as compared to control group mice (**Figure S1B-D**). Administration of sertraline, a commonly used antidepressant, significantly alleviated this fear response. Consistent with this result, in the open field test we found that foot-shock exposure largely reduced the time and distance of locomotion in the center area (**Figure S1E-H**) and administration of sertraline rescued this phenomenon. Together, these findings indicated that the electric foot-shock model was sufficient to induce PTSD in mice.

In order to study changes in immunocytes from the brains of PTSD mice, we utilized CyTOF technology to dissect immunocytes distributions in control and PTSD mice (**Figure 1A**). Five mouse brain samples each from control or PTSD groups were mixed and labeled with CD45 antibodies conjugated with 42 different isotope-labeled antibodies, including immunocyte-specific and some functional markers (**Supplementary Table 1**). The immunocytes were categorized into different clusters according to the expression profiles of marker genes (**Figure 1B and C**). Consistent with previous reports, multiple immune cell types were identified in naïve mouse brains, including microglia ( $CD11b^+CD45^{low}CX3CR1^+F4/80^+$ ) and various  $CD45^{high}$  cells, such as  $CD4^+$  T cells ( $CD45^{high}TCR-\beta^+CD4^+$ ),  $CD8^+$  T cells ( $CD45^{high}TCR-\beta^+CD4^+$ ), type A dendritic cells (DCs -  $CD45^{high}CD11c^+CD11b^+$ ), type B DCs ( $CD45^{high}CD11c^+CD11b^-$ ),  $Gr-1^+$  myeloid cells ( $CD45^{high}CD11b^+Gr-1^+$ ), monocytes ( $CD45^{high}CD11b^+Ly6C^+$ ) and eosinophils ( $CD45^{high}CD11b^+CD24^+CD44^+siglec-F^+$ ). Importantly, we found that more than 70% of these immune cells were microglia (**Figure 1D**). Moreover, the immune homeostasis was disrupted in the brains of PTSD mice, characterized by the increased ratio of microglia/immunocytes. This suggested that microglia were the cells that responded to the development of PTSD in mice. Together, these results show that microglia were the dominant immune cell type in the mouse brains and were produced in higher numbers in response to development of PTSD.

To further define the number and morphology changes in microglia during PTSD development, *Cx3cr1-GFP* mice were utilized. The PFC, HP and AMY have been reported to be the major brain regions involved in PTSD development, therefore we examined the changes in microglia from these brain regions at different time points. The number of microglia in the PFC was significantly increased upon delivering foot-shocks, with the highest levels on day 5 and increasing trends on days 10 and 17 (**Figure 2A and B**). In the HP, the number of microglia increased on day 5, but quickly recovered on day 10 (**Figure 2C**). However, the number of microglia in AMY showed no significant changes (**Figure 2D**). These results suggest that microglial numbers are altered in a time- and brain region-dependent manner during the progression of PTSD.

### **Dynamic alterations of microglial status throughout PTSD development**

Given that microglial activation is always accompanied by dynamic changes in morphology<sup>36</sup>, we examined whether microglial morphology was changed in PTSD condition. Foot-shock exposure significantly altered the microglial morphology in the PFC and HP, characterized by enlarged soma area, reduced branch length and reduced arborization (**Figure 2E-2H**), especially on day 5 (**Figure 2F-H**). However, in AMY, the microglia showed only slight changes. These observations suggest that changes in microglial morphology also occur in a time- and region-specific manner.

Next, we examined the gene expression profiles during PTSD progression. Foot-shocks exposure did not change the expression profiles of the PFC and AMY (**Figure 2I-2K**). However, there were dramatic alterations in the HP, with significant increases of IL-1 $\beta$ , IL-6, TNF- $\alpha$  and interferon- $\gamma$  (IFN- $\gamma$ ). Thus, we were able to demonstrate region-specific alterations of microglial gene expression during PTSD progression.

### **Genetic/pharmacological depletion of Microglia alleviated PTSD-like symptoms in mice**

The depletion of microglia in murine brains has been effectively performed in multiple previous studies, providing an effective way to study the role of microglia *in vivo*<sup>31,37</sup>. We used *Cx3cr1<sup>creER</sup>:iDTR* mice administered with tamoxifen to express the diphtheria toxin receptor (DTR) specifically in microglia. We then administered diphtheria toxin (DT) to deplete microglia in the central nervous system while leaving other CX3CR1<sup>+</sup> populations intact (**Figure 3A**). To examine the efficiency of microglial deletion, brain slices were stained by IBA1 antibody 3 days after the first DT administration and saw that about 90% of microglia in the brain had been removed (**Figure 3B and 3C**). We found that in the PTSD model microglial deletion group mice significantly reduced the freezing time in the contextual recall test as compared to the control group (**Figure 3D-G**). In the open field test, in the PTSD model microglial deletion group mice increased the time spent and the distance traveled in the central zone (**Figure 3H-K**). Meanwhile, in the EPM test, in the PTSD model microglial deletion group mice increased the percentage of open arm entries, the percentage of time spent in open arms and the percentage of open arm distance travelled (**Figure 3L-O**). Collectively, these results suggest that microglial deletion after foot-shocks delivery alleviates PTSD related behaviors in mice.

It has been reported that a genetically ablated microglial population can be restored within 2 weeks of deletion<sup>38,39</sup>. In our research we found that microglia repopulated within 14 days after DT treatment, therefore microglial number was actually restored when we performed the behavior tests (open field test and elevated plus maze test) (**Figure S3A and S3B**). This raises the question of whether the observed improvement in PTSD symptoms is due to deletion or repopulation of microglia. To address this question, a chemical compound, PLX3397, which has been reported to effectively delete microglia, was orally administered to mice for 3 weeks<sup>40</sup>. The mice then received foot-shocks and underwent behavior tests. The compound PLX3397 was continually administered until all the behavior tests were completed, to sustain the deletion of microglia (**Figure S3C and S3D**). We found that deletion of microglia by administration of PLX3397 significantly decreased the contextual fear freezing time (**Figure S3E-G**), increased the time spent and the distance traveled in the central zone (**Figure S3H-K**), and slightly improved the activity in open arms in the EPM test (**Figure S3L-S3O**). These results reveal that microglial depletion alleviates PTSD-like behaviors in mice, implicating microglial activation in the development of PTSD-like phenotypes.

In order to further reveal the mechanism of microglia deletion alleviates PTSD symptoms, we performed mass cytometry experiments and examined the alteration of microglial status among wildtype group mice, foot-shocks group mice, microglial deletion group mice and microglial deletion with foot-shocks group mice. Microglial subtypes were gated as Cx3cr1<sup>+</sup>CD11b<sup>+</sup>CD45<sup>low</sup> population (**Figure 4A**), and microglial subtypes were further categorized by FlowSOM-guided clustering according to the expression profiles of marker genes and showed in a t-SNE map (**Figure 4B and 4C**). Microglial deletion significantly altered the microglial patterns (**Figure 4D**). Similar to the result that has been reported before<sup>39</sup>, the ratio of Ki67<sup>+</sup> microglia was markedly increased in the microglial deletion groups (**Figure 4E**), indicating that the repopulated microglia was due to the high proliferation. We further analyzed the expression levels of functional markers, including CD172, iNOS and CD38, which were increased by foot-shocks treatment (**Figure 4F-H**). Interestingly, microglia deletion significantly downregulates the genes expression under foot-shocks (black bar vs blue bar in **Figure 4F-H**). Together, these results indicate that microglial depletion alleviates PTSD-like symptoms by reducing microglia-associated inflammation.

### **Inhibition of microglial activation by minocycline alleviates PTSD-like symptoms**

To further illustrate the role of microglial activation and neuroinflammation, we examined the effect of minocycline, a drug that suppresses microglial activation, on PTSD symptoms<sup>21</sup>. We analyzed the changes in microglial morphology and gene expression profiles in the HP. Treatment with minocycline suppressed the microglial activation induced by foot-shock exposure, characterized by increased branch number and branch length, and decreased expression of pro-inflammatory cytokines like IL-1b, IL-6 and TNF-a (**Figure 5A and B**). Furthermore, the behavior tests showed that minocycline administration decreased fear contextual response (**Figure 5C-E**), improved performance in the open field test (**Figure 5F-I**), and increased activity in open arms in the EPM test (**Figure 5J-M**). Overall, these results suggest that suppression of microglial activation can alleviate PTSD-like behaviors induced by foot-shock exposure.

## Discussion

Previous studies on the development of PTSD mainly focused on abnormalities of neuronal function, such as dysregulation of neural circuits and damaged brain structures<sup>41,42</sup>. Thus, the involvement and role of non-neuronal cells during PTSD remains largely undefined. In this study, we found that PTSD development alters the activation of microglia in certain brain regions. This temporal and spatial alteration of microglial cells during the development of PTSD provides a direct link between microglial activation and mental disorders. Importantly, microglial depletion or inhibition alleviated PTSD-like behaviors, implying that targeting microglia to counter neuroinflammation offers a potential therapeutic avenue for PTSD (**Figure 6**).

Currently, there is no standard murine model of PTSD, even some putative models could mimic one or more symptoms of PTSD, among which electronic foot-shocks is extensively used in this field. In this model, the stimuli consist of physical and emotional factors, which could reproduce the core symptoms of PTSD including avoidance, hyperarousal, anxiety and re-experiencing. Importantly, the electronic foot-shocks model can be integrated with other behavior tests for extended study on PTSD symptoms<sup>43,44</sup>. By using this model, we successfully observed the core symptoms of anxiety and fear responses. The reduced dendritic spine has been reported as a potential synaptic marker for PTSD<sup>45</sup>, but we had not examined it in this work. Accordingly, electronic foot-shocks model have been used in our study.

In this study, we used only age-matched male mice for the experiments. Previous reports showed that there is gender difference in mice under foot-shock stress treatment<sup>46,47</sup>. The reason that the female mice are not usually used might be the anti-inflammatory activity of estrogen<sup>48</sup>. Therefore, the majority of psychiatry and neurology related studies, the male mice were generally used<sup>20,49</sup>.

Mass cytometry is a new method in single cell resolution offers broad, high-dimensional perspective of the immunological milieu in brain. Our findings with the help of mass cytometry were consistent with previous report, the percentage of microglia was 70-80% in naïve brain<sup>28</sup>. In Dunja's study, they identify different subsets of myeloid cells and the phenotypic changes in CNS immune cells during aging and central nervous disease condition<sup>29</sup>. Our work found that in PTSD condition, microglia were globally affected, while only a subset of microglia was significantly altered in neurodegenerative disease. Beside microglia response to chronic stress, we also found other immunocytes changed in this process. Changed DCs, CD4+ and CD8+ T cells may play a role in PTSD pathogenesis. As reported before, CD4+ derived xanthine acts on the oligodendrocytes and triggers onset of anxiety, Dendritic cells involved in major depression pathogenesis though remodeling of D1 neurons by RhoA/Rho-kinase<sup>50,51</sup>.

The finding that short-term stress exposure results in hippocampal microglia activation was consistent with previous report that acute-tail-shock results in microglia proliferation and activation<sup>52</sup>. It has been reported that the number of microglia in HP increases due to proliferation and activation in the acute phase of major depression, and drops due to apoptosis in the later stages of major depression<sup>20</sup>. However, in our model, we failed to see microglial apoptosis, which could be attributed to the short

duration of stress exposure. Microglial morphology changes have also been demonstrated in ischemic stroke and reperfusion processes<sup>53</sup>, but parallel analyses of gene expression were not performed in these studies. In our study, we present an analysis of microglia morphology and gene expression profiles throughout the development of PTSD. Recently, several studies have demonstrated the spatial and temporal heterogeneity of microglia<sup>18,54,55</sup>, pointing to a functional relevance of diversity in microglial morphology in the brain. The present study confirms specific temporal and spatial activation of microglia in affected brain regions during PTSD progression, which may be underpinned by different gene expression patterns.

The finding that DTR/DT-mediated microglial depletion significantly decreased contextual fear memory and alleviated anxiety-like behavior were consistent with previous study that microglia depletion results in learning and memory deficits<sup>31</sup>. Depletion of microglia is a useful method to study microglial functions *in vivo*. In contrast to the herpes simplex virus thymidine kinase/ ganciclovir (HSVTK/GCV) system, the DTR/DT system specifically deletes microglia without inflicting damage upon the blood brain barrier<sup>56</sup>. In this study, it is benefit for PTSD treatment, but this strategy is cannot be adopted for human patients. However, minocycline might provide an alternative treatment option for PTSD patients, since we found that minocycline effectively attenuates PTSD behaviors in the acute phase. The effect of minocycline on PTSD pathogenesis corroborates the results of previous studies demonstrating the same phenomenon using acute major depression model and Alzheimer's disease model<sup>20,57</sup>

In our work, the genetic deletion (DTR/DT) and pharmacological deletion (PLX3997) were utilized for microglia deletion, both of them alleviates PTSD behaviors in mice. Recently, several studies have reported microglia repopulation have the benefit effect following brain injury or reverses brain function deficits in aged mice<sup>58,59</sup>. In our hands, we also observed that DTR/DT's shows a more significant improvement than PLX3997, indicating along with the microglial deletion-mediated neuroinflammation inhibition, microglia repopulation probably also contribute to PTSD alleviation via some unappreciated mechanism.

Microglia are the primary cellular responders to stress, releasing various inflammatory cytokines upon stress exposure. In accordance with our observations, it has also been reported that neural inflammation accompanies major depressive disorder<sup>60-62</sup>. However, it is still puzzling how microglial activation and neural inflammation alter neuronal functions. It has been proposed that IL-1 $\beta$ , IL-6 and TNF $\alpha$  can directly modulate neuronal plasticity and cause mood disorders<sup>63-65</sup>. Another possibility is that the increased microglia number could enhance synaptic trimming and it is known that synapse loss underpins mood disorders<sup>66</sup>. Importantly, microglia-driven microenvironments are critical for neurogenesis and neuronal function and hence, it is possible that stress-induced microglial activation might lead to the development of PTSD.

## Conclusion

Our results demonstrated microglia are the major brain immune cells respond to PTSD, microglial activation play a critical role in PTSD development. microglial inhibition is a potential therapeutic strategy for the clinical treatment of PTSD.

## Abbreviations

PTSD

post-traumatic stress disorder

TNF $\alpha$

tumor necrosis factor $\alpha$

IL-6

interleukin-6

IL-1 $\beta$

interleukin-1 $\beta$

CNS

central nervous system

5-HT

5-hydroxytryptamine

PFC

prefrontal cortex HP:hippocampus

AMY

amygdala

CyTOF

Cytometry by Time-Of-Flight

EPM

elevated plus maze

IFN- $\gamma$

interferon- $\gamma$

DTR

diphtheria toxin receptor

## Declarations

### Ethics approval and consent to participate

All animal experiments were approved by the Institutional Animal Care and Use Committee at Beijing Institute of Basic Medical Sciences.

### Consent for publication

Not applicable

## Availability of data and materials

All data generated or analysed during this study are included in this published article and its supplementary information files.

## Conflict of Interest statement

The authors declare that they have no competing interests.

## Funding

This work was supported by grants from the National Natural Science Foundation of China (No. 81930029 and 81630026 to ZY, No. 81870839 to JC, No. 31600946 to SW and No. 81701187 to YL), The National Major Project of Support Program (Grant 2019-JCJQ-ZD-195 and No. 16CXZ028 to ZY), and the Key Field Research and Development Program of Guangdong Province (2018B030337001).

## Authors' contributions:

Shuoshuo Li performed all the experiments and wrote the manuscript. Yajin Liao gave some help in the behavior test and suggestions. Yuan Dong and Xiaoheng Li provided some help in analyzing the data and suggestions. Jun Li helped to generate transgene mice. Yong Cheng gave some help in mass cytometry. Jinbo Cheng and Zengqiang Yuan supervised this project.

## Acknowledgement:

We thank Dr. Junwei Hao (Tianjin Medical University, Tianjin, China) for gifting *Cx3cr1-GFP* mice.

## References

1. Bam M, et al. Dysregulated immune system networks in war veterans with PTSD is an outcome of altered miRNA expression and DNA methylation. *Scientific reports*. 2016;6:31209. doi:10.1038/srep31209.
2. Gola H, et al. Posttraumatic stress disorder is associated with an enhanced spontaneous production of pro-inflammatory cytokines by peripheral blood mononuclear cells. *BMC Psychiatry*. 2013;13:40. doi:10.1186/1471-244x-13-40.
3. Jergovic M, et al. Patients with posttraumatic stress disorder exhibit an altered phenotype of regulatory T cells. *Allergy, asthma, and clinical immunology*. official journal of the Canadian Society of Allergy Clinical Immunology. 2014;10:43. doi:10.1186/1710-1492-10-43.
4. Zhou J, et al. Dysregulation in microRNA expression is associated with alterations in immune functions in combat veterans with post-traumatic stress disorder. *PloS one*. 2014;9:e94075. doi:10.1371/journal.pone.0094075.

5. Passos IC, et al. Inflammatory markers in post-traumatic stress disorder: a systematic review, meta-analysis, and meta-regression. *Lancet Psychiatry*. 2015;2:1002–12. doi:10.1016/s2215-0366(15)00309-0.
6. Eraly SA, et al. Assessment of plasma C-reactive protein as a biomarker of posttraumatic stress disorder risk. *JAMA psychiatry*. 2014;71:423–31. doi:10.1001/jamapsychiatry.2013.4374.
7. Pan RY, et al. Sodium rutin ameliorates Alzheimer's disease-like pathology by enhancing microglial amyloid-beta clearance. *Sci Adv*. 2019;5:eaau6328. doi:10.1126/sciadv.aau6328.
8. Cheng J, et al. Autophagy regulates MAVS signaling activation in a phosphorylation-dependent manner in microglia. *Cell death differentiation*. 2017;24:276–87. doi:10.1038/cdd.2016.121.
9. Zhao S, et al. Hippo/MST1 signaling mediates microglial activation following acute cerebral ischemia-reperfusion injury. *Brain Behav Immun*. 2016;55:236–48. doi:10.1016/j.bbi.2015.12.016.
10. Rial D, et al. Depression as a Glial-Based Synaptic Dysfunction. *Front Cell Neurosci*. 2015;9:521. doi:10.3389/fncel.2015.00521.
11. Muhie S, et al. Brain transcriptome profiles in mouse model simulating features of post-traumatic stress disorder. *Mol Brain*. 2015;8:14. doi:10.1186/s13041-015-0104-3.
12. Zhao X, et al. Behavioral, inflammatory and neurochemical disturbances in LPS and UCMS-induced mouse models of depression. *Behav Brain Res*. 2017. doi:10.1016/j.bbr.2017.05.064.
13. Reichenberg A, et al. Cytokine-associated emotional and cognitive disturbances in humans. *Arch Gen Psychiatry*. 2001;58:445–52.
14. Li M, et al. Lentivirus-mediated interleukin-1beta (IL-1beta) knock-down in the hippocampus alleviates lipopolysaccharide (LPS)-induced memory deficits and anxiety- and depression-like behaviors in mice. *J Neuroinflammation*. 2017;14:190. doi:10.1186/s12974-017-0964-9.
15. Tynan RJ, et al. A comparative examination of the anti-inflammatory effects of SSRI and SNRI antidepressants on LPS stimulated microglia. *Brain Behav Immun*. 2012;26:469–79. doi:10.1016/j.bbi.2011.12.011.
16. Nimmerjahn A, Kirchhoff F, Helmchen F. Resting microglial cells are highly dynamic surveillants of brain parenchyma in vivo. *Science*. 2005;308:1314–8. doi:10.1126/science.1110647.
17. Davalos D, et al. ATP mediates rapid microglial response to local brain injury in vivo. *Nat Neurosci*. 2005;8:752–8. doi:10.1038/nn1472.
18. Lawson LJ, Perry VH, Dri P, Gordon S. Heterogeneity in the distribution and morphology of microglia in the normal adult mouse brain. *Neuroscience*. 1990;39:151–70.
19. de Haas AH, Boddeke HW, Biber K. Region-specific expression of immunoregulatory proteins on microglia in the healthy CNS. *Glia*. 2008;56:888–94. doi:10.1002/glia.20663.
20. Kreisel T, et al. Dynamic microglial alterations underlie stress-induced depressive-like behavior and suppressed neurogenesis. *Mol Psychiatry*. 2014;19:699–709. doi:10.1038/mp.2013.155.
21. 10.1093/cercor/bhs151

- Hinwood M, et al. Chronic stress induced remodeling of the prefrontal cortex: structural reorganization of microglia and the inhibitory effect of minocycline. *Cerebral cortex (New York, N.Y.: 1991)* **23**, 1784–1797, doi:10.1093/cercor/bhs151 (2013).
22. Hultman R, et al. Dysregulation of Prefrontal Cortex-Mediated Slow-Evolving Limbic Dynamics Drives Stress-Induced Emotional Pathology. *Neuron*. 2016;91:439–52. doi:10.1016/j.neuron.2016.05.038.
23. Ye X, Kapeller-Libermann D, Travaglia A, Inda MC, Alberini CM. Direct dorsal hippocampal-prelimbic cortex connections strengthen fear memories. *Nat Neurosci*. 2017;20:52–61. doi:10.1038/nn.4443.
24. Adhikari A, et al. Basomedial amygdala mediates top-down control of anxiety and fear. *Nature*. 2015;527:179–85. doi:10.1038/nature15698.
25. Hayes JP, Vanelzakker MB, Shin LM. Emotion and cognition interactions in PTSD: a review of neurocognitive and neuroimaging studies. *Front Integr Neurosci*. 2012;6:89. doi:10.3389/fnint.2012.00089.
26. Shin LM, et al. Regional cerebral blood flow in the amygdala and medial prefrontal cortex during traumatic imagery in male and female Vietnam veterans with PTSD. *Arch Gen Psychiatry*. 2004;61:168–76. doi:10.1001/archpsyc.61.2.168.
27. Spitzer MH, Nolan GP, Mass Cytometry. Single Cells, Many Features. *Cell*. 2016;165:780–91. doi:10.1016/j.cell.2016.04.019.
28. Korin B, et al. High-dimensional, single-cell characterization of the brain's immune compartment. *Nat Neurosci*. 2017;20:1300–9. doi:10.1038/nn.4610.
29. 10.1016/j.immuni.2018.01.011  
Mrdjen D, et al. High-Dimensional Single-Cell Mapping of Central Nervous System Immune Cells Reveals Distinct Myeloid Subsets in Health, Aging, and Disease. *Immunity* **48**, 380–395 e386, doi:10.1016/j.immuni.2018.01.011 (2018).
30. Ajami B, et al. Single-cell mass cytometry reveals distinct populations of brain myeloid cells in mouse neuroinflammation and neurodegeneration models. *Nat Neurosci*. 2018;21:541–51. doi:10.1038/s41593-018-0100-x.
31. Parkhurst CN, et al. Microglia promote learning-dependent synapse formation through brain-derived neurotrophic factor. *Cell*. 2013;155:1596–609. doi:10.1016/j.cell.2013.11.030.
32. 10.1155/2012/623753  
Zhang LM, et al. Anxiolytic effects of flavonoids in animal models of posttraumatic stress disorder. *Evidence-based complementary and alternative medicine: eCAM* 2012, 623753, doi:10.1155/2012/623753 (2012).
33. Qiu ZK, et al. Repeated administration of AC-5216, a ligand for the 18 kDa translocator protein, improves behavioral deficits in a mouse model of post-traumatic stress disorder. *Prog Neuropsychopharmacol Biol Psychiatry*. 2013;45:40–6. doi:10.1016/j.pnpbp.2013.04.010.
34. Zhang X-Y, et al. The 18 kDa Translocator Protein (TSPO) Overexpression in Hippocampal Dentate Gyrus Elicits Anxiolytic-Like Effects in a Mouse Model of Post-traumatic Stress Disorder. *Front Pharmacol*. 2018;9:1364–4. doi:10.3389/fphar.2018.01364.

35. 10.4049/jimmunol.1402661  
Mei HE, Leipold MD, Schulz AR, Chester C, Maecker HT. Barcoding of live human peripheral blood mononuclear cells for multiplexed mass cytometry. *Journal of immunology (Baltimore, Md.: 1950)* **194**, 2022–2031, doi:10.4049/jimmunol.1402661 (2015).
36. Caetano L, et al. Adenosine A2A receptor regulation of microglia morphological remodeling-gender bias in physiology and in a model of chronic anxiety. *Mol Psychiatry*. 2017;22:1035–43. doi:10.1038/mp.2016.173.
37. Asai H, et al. Depletion of microglia and inhibition of exosome synthesis halt tau propagation. *Nat Neurosci*. 2015;18:1584–93. doi:10.1038/nn.4132.
38. Bruttger J, et al. Genetic Cell Ablation Reveals Clusters of Local Self-Renewing Microglia in the Mammalian Central Nervous System. *Immunity*. 2015;43:92–106. doi:10.1016/j.immuni.2015.06.012.
39. Huang Y, et al. Repopulated microglia are solely derived from the proliferation of residual microglia after acute depletion. *Nat Neurosci*. 2018;21:530–40. doi:10.1038/s41593-018-0090-8.
40. Szalay G, et al. Microglia protect against brain injury and their selective elimination dysregulates neuronal network activity after stroke. *Nature communications*. 2016;7:11499. doi:10.1038/ncomms11499.
41. Guo N, et al. Dentate granule cell recruitment of feedforward inhibition governs engram maintenance and remote memory generalization. *Nat Med*. 2018;24:438–49. doi:10.1038/nm.4491.
42. Bennett MR, Hatton SN, Lagopoulos J. Stress, trauma and PTSD: translational insights into the core synaptic circuitry and its modulation. *Brain Struct Funct*. 2016;221:2401–26. doi:10.1007/s00429-015-1056-1.
43. Bali A, Jaggi AS. Electric foot shock stress: a useful tool in neuropsychiatric studies. *Rev Neurosci*. 2015;26:655–77. doi:10.1515/revneuro-2015-0015.
44. 10.1007/978-1-4939-9554-7\_19  
Zhang L, et al. Updates in PTSD Animal Models Characterization. *Methods in molecular biology (Clifton, N.J.)* 2011, 331–344, doi:10.1007/978-1-4939-9554-7\_19 (2019).
45. Smith KL, et al. Microglial cell hyper-ramification and neuronal dendritic spine loss in the hippocampus and medial prefrontal cortex in a mouse model of PTSD. *Brain Behav Immun*. 2019;80:889–99. doi:10.1016/j.bbi.2019.05.042.
46. Chester JA, Barrenha GD, Hughes ML, Keuneke KJ. Age- and sex-dependent effects of footshock stress on subsequent alcohol drinking and acoustic startle behavior in mice selectively bred for high-alcohol preference. *Alcohol Clin Exp Res*. 2008;32:1782–94. doi:10.1111/j.1530-0277.2008.00763.x.
47. Day HLL, Reed MM, Stevenson CW. Sex differences in discriminating between cues predicting threat and safety. *Neurobiol Learn Mem*. 2016;133:196–203. doi:10.1016/j.nlm.2016.07.014.
48. Villa A, et al. Sex-Specific Features of Microglia from Adult Mice. *Cell reports*. 2018;23:3501–11. doi:10.1016/j.celrep.2018.05.048.

49. McKim DB, et al. Microglial recruitment of IL-1beta-producing monocytes to brain endothelium causes stress-induced anxiety. *Mol Psychiatry*. 2018;23:1421–31. doi:10.1038/mp.2017.64.
50. Fox ME, et al. Dendritic remodeling of D1 neurons by RhoA/Rho-kinase mediates depression-like behavior. *Mol Psychiatry*. 2018. doi:10.1038/s41380-018-0211-5.
51. Fan KQ, et al. Stress-Induced Metabolic Disorder in Peripheral CD4(+) T Cells Leads to Anxiety-like Behavior. *Cell*. 2019;179:864–79.e819. doi:10.1016/j.cell.2019.10.001.
52. Frank MG, Baratta MV, Sprunger DB, Watkins LR, Maier SF. Microglia serve as a neuroimmune substrate for stress-induced potentiation of CNS pro-inflammatory cytokine responses. *Brain Behav Immun*. 2007;21:47–59. doi:10.1016/j.bbi.2006.03.005.
53. Morrison HW, Filosa JA. A quantitative spatiotemporal analysis of microglia morphology during ischemic stroke and reperfusion. *J Neuroinflammation*. 2013;10:4. doi:10.1186/1742-2094-10-4.
54. Grabert K, et al. Microglial brain region-dependent diversity and selective regional sensitivities to aging. *Nat Neurosci*. 2016;19:504–16. doi:10.1038/nn.4222.
55. Masuda T, et al. Spatial and temporal heterogeneity of mouse and human microglia at single-cell resolution. *Nature*. 2019;566:388–92. doi:10.1038/s41586-019-0924-x.
56. Waisman A, Ginhoux F, Greter M, Bruttger J. Homeostasis of Microglia in the Adult Brain: Review of Novel Microglia Depletion Systems. *Trends Immunol*. 2015;36:625–36. doi:10.1016/j.it.2015.08.005.
57. Amani M, Shokouhi G, Salari AA. Minocycline prevents the development of depression-like behavior and hippocampal inflammation in a rat model of Alzheimer's disease. *Psychopharmacology*. 2019;236:1281–92. doi:10.1007/s00213-018-5137-8.
58. Rice RA, et al. Microglial repopulation resolves inflammation and promotes brain recovery after injury. *Glia*. 2017;65:931–44. doi:10.1002/glia.23135.
59. Elmore MRP, et al. Replacement of microglia in the aged brain reverses cognitive, synaptic, and neuronal deficits in mice. *Aging cell*. 2018;17:e12832. doi:10.1111/acer.12832.
60. Haroon E, Raison CL, Miller AH. Psychoneuroimmunology meets neuropsychopharmacology: translational implications of the impact of inflammation on behavior. *Neuropsychopharmacology*. 2012;37:137–62. doi:10.1038/npp.2011.205.
61. Dantzer R, O'Connor JC, Freund GG, Johnson RW, Kelley KW. From inflammation to sickness and depression: when the immune system subjugates the brain. *Nat Rev Neurosci*. 2008;9:46–56. doi:10.1038/nrn2297.
62. Blank T, Prinz M. Microglia as modulators of cognition and neuropsychiatric disorders. *Glia*. 2013;61:62–70. doi:10.1002/glia.22372.
63. Lewitus GM, et al. Microglial TNF-alpha Suppresses Cocaine-Induced Plasticity and Behavioral Sensitization. *Neuron*. 2016;90:483–91. doi:10.1016/j.neuron.2016.03.030.
64. Liu Y, et al. TNF-alpha Differentially Regulates Synaptic Plasticity in the Hippocampus and Spinal Cord by Microglia-Dependent Mechanisms after Peripheral Nerve Injury. *J Neurosci*. 2017;37:871–81. doi:10.1523/jneurosci.2235-16.2016.

65. Patterson SL. Immune dysregulation and cognitive vulnerability in the aging brain: Interactions of microglia, IL-1beta, BDNF and synaptic plasticity. *Neuropharmacology*. 2015;96:11–8. doi:10.1016/j.neuropharm.2014.12.020.
66. Wohleb ES, Terwilliger R, Duman CH, Duman RS. Stress-Induced Neuronal Colony Stimulating Factor 1 Provokes Microglia-Mediated Neuronal Remodeling and Depressive-like Behavior. *Biol Psychiatry*. 2018;83:38–49. doi:10.1016/j.biopsych.2017.05.026.

## Figures

Figure 1

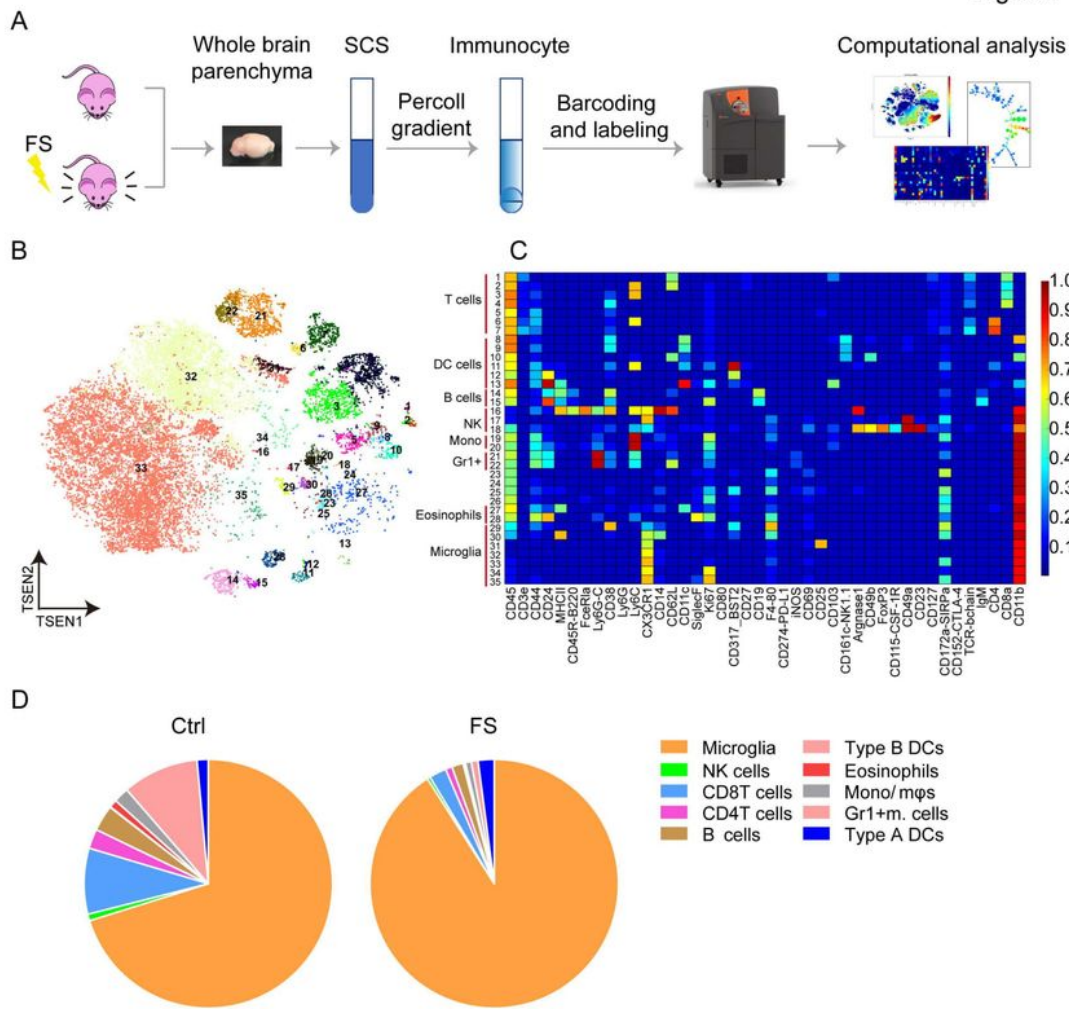
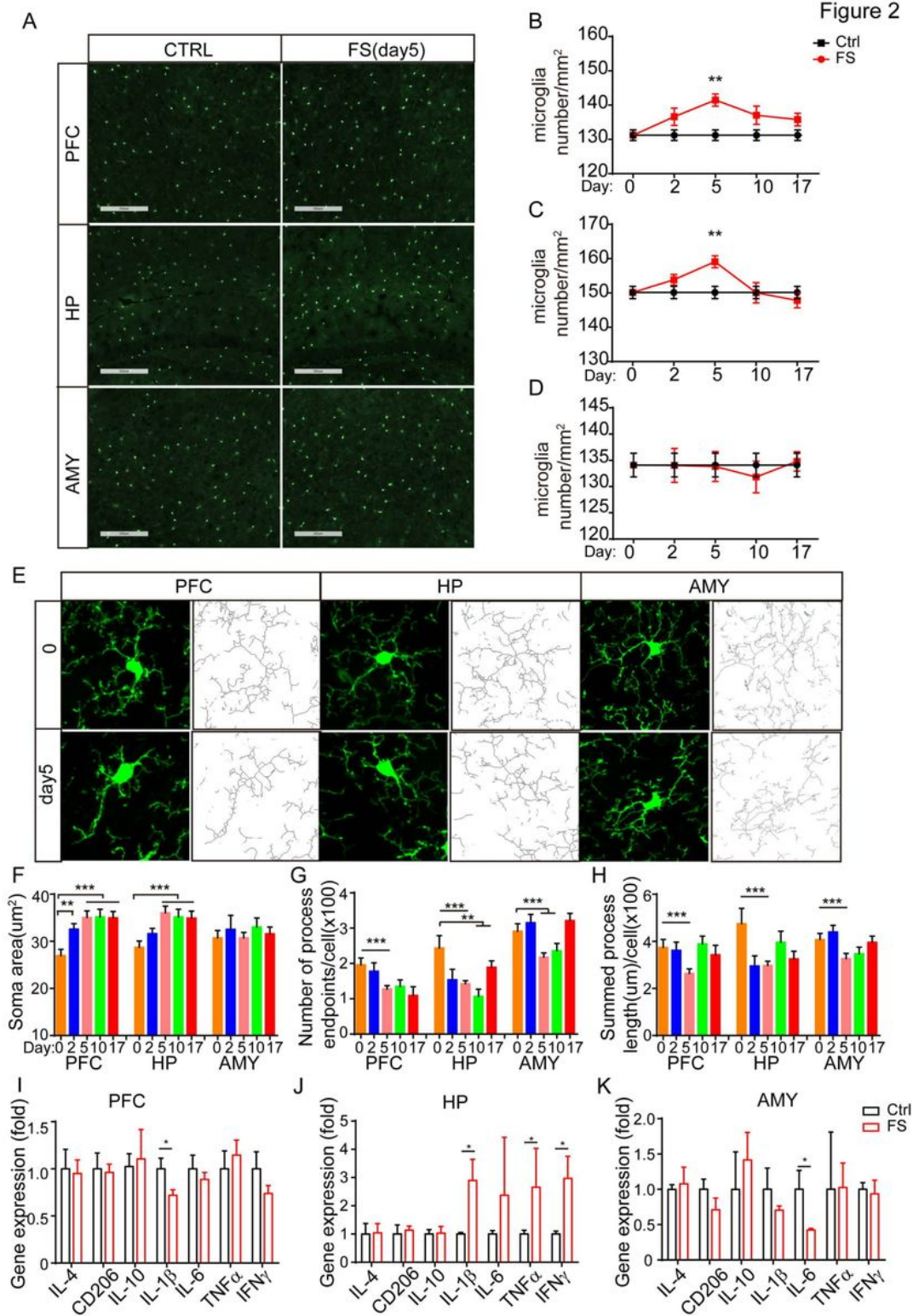


Figure 1

Identification and characterization of immunocyte populations in mouse brains by mass cytometry. (A) Schematic of mass cytometry procedure. In each group, brains were separated from five mice, dissociated into single cell suspensions, mixed as a single sample, barcoded, pooled and stained with metal-tagged primary antibodies. The samples were analyzed by the CyTOF machine and immunocyte populations were identified and characterized using visualization tool for statistical epistasis networks

(viSNE) and heatmap analysis. (B) viSNE map displaying immune cells from control mice. Colors represent different cell populations clustered by Flow Self Organizing Map (FlowSOM). (C) Clustering and expression level of functional markers in immunocytes from naïve brains. (D) Frequency distributions of immunocytes in control and PTSD model brains. (FS: foot shocks, SCS: single cell solution)



**Figure 2**

Dynamic alterations of microglial status in PTSD development. (A) Representative picture of microglia density in different brain areas of Cx3cr1-GFP transgenic mice of the control and foot-shock groups; scale bar = 200  $\mu$ m. (B) Microglial density alterations during PTSD development in PFC area (n = 3-4 for each group). (C) Microglial density alterations during PTSD development in HP area (n = 3-4 for each group). (D) Microglial density alterations during PTSD development in AMY area (n = 3-4 for each group). (E) Representative image of microglia morphology and skeletonized inset in different brain areas of Cx3cr1-GFP transgenic mice at different time points after foot-shock exposure, scale bar = 10  $\mu$ m. (F) Statistical analysis of microglial soma area from different brain regions at different time points (n = 3-4 mice for each group, 50 cells were analyzed per mouse). (G) Microglial process end points/cell (n = 3-4 mice for each group, 50 cells were analyzed per mouse). (H) Microglial process lengths (n = 3-4 mice for each group, 50 cells were analyzed per mouse). Data are expressed as mean  $\pm$  SEM, \* p < 0.05, \*\* p < 0.01, \*\*\* p < 0.001 for indicated cooperation (ANOVA). (I) Effects of PTSD on the mRNA expression levels of neuroinflammatory genes in PFC, (J) HP and (K) AMY on day 5; \* p < 0.05 (Student's t-test). (PFC: prefrontal cortex HP: hippocampus AMY: amygdala)

Figure 3

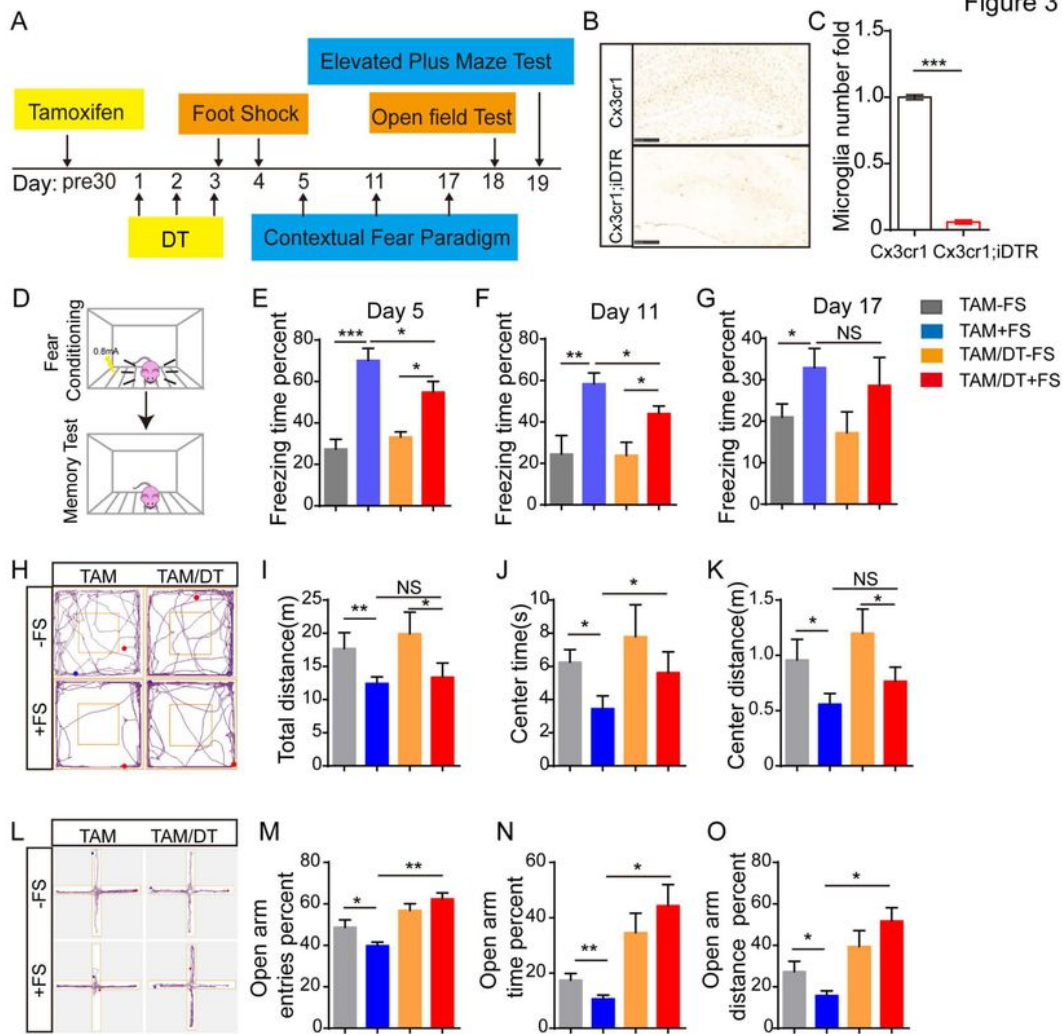
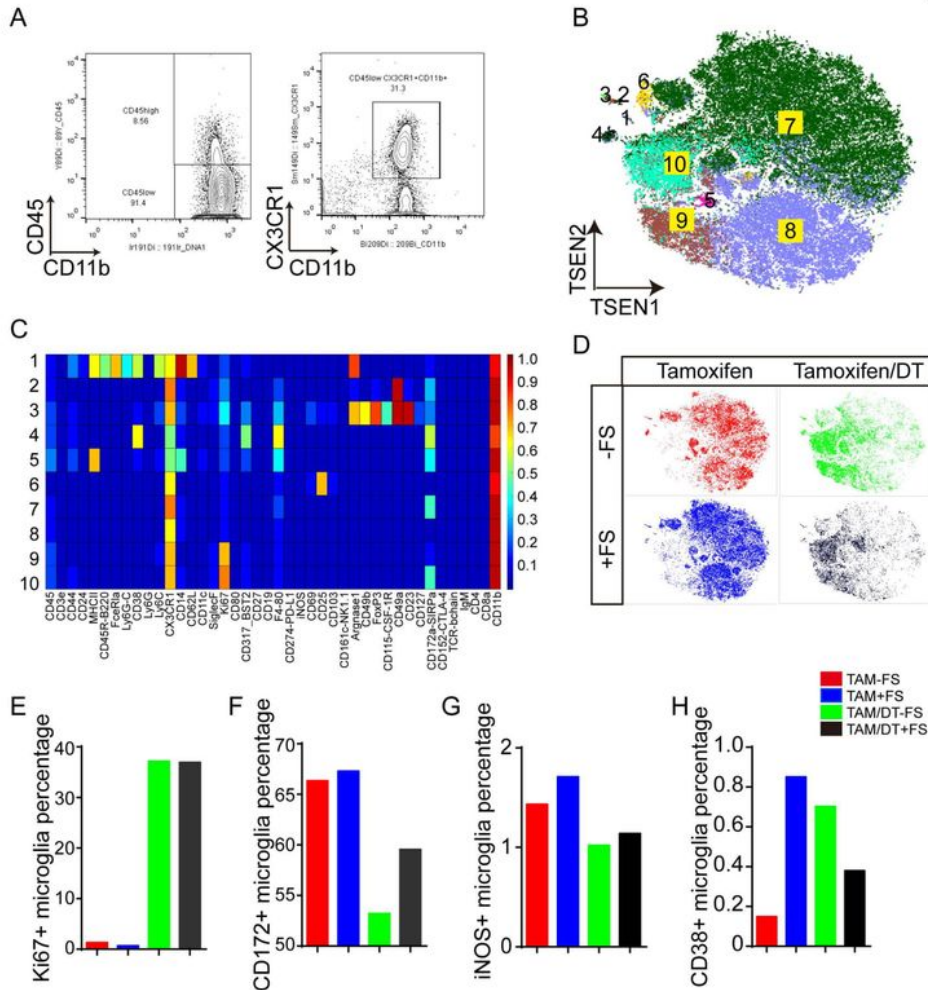


Figure 3

Microglial depletion alleviates PTSD symptoms. (A) Schematic representation of experimental procedure. Tamoxifen were administrated 30 days before DT injection. DT was intraperitoneally injected on -TAM+DT+FS mice, and Saline was injected as a control on -TAM-DT+FS mice. At day3, day4, foot-shocks were delivered to mice. At day5, 11, 17 contextual fear recall test were performed. At day18, open field test were performed. At day19, elevated plus maze test were performed. (B) IHC staining shows microglia

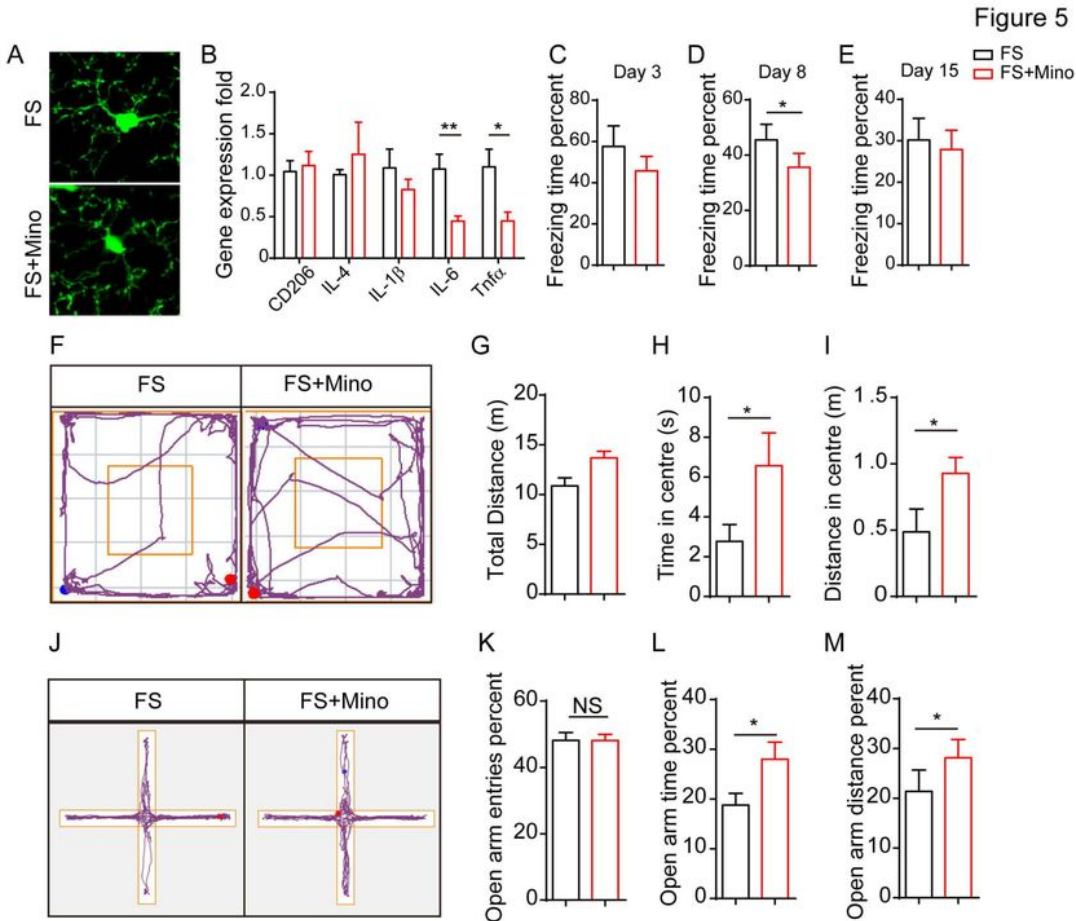
depletion efficiency after DT injection 3days. (C) Statistic data shows microglia number decreased after DT injection. \*\*\*  $p < 0.001$  (Student's t-test). (D) Representative foot-shock delivery and contextual fear freezing test methods. (E-G) Effect of microglial deletion on foot-shock induced contextual fear freezing test. (H) Representative image of mouse track plots in open field test. (I-K) Statistical analysis of mouse performance in open field test. (L) Representative image of mouse track plots in EPM test. (M-O) Statistical analysis of mouse performance in EPM test;  $n = 10$ , data are expressed as means  $\pm$  SEM, \*  $p < 0.05$ , \*\*  $p < 0.01$ , \*\*\*  $p < 0.001$  (ANOVA). (DT: diphtheria toxin, TAM: Tamoxifen, NS: no significant)

Figure 4



## Figure 4

Microglial depletion alleviates PTSD-like symptoms by changing the whole microglial status. (A) Microglia were gated as CD11b+CD45lowCX3CR1+ cells. (B) viSNE map displaying microglia subtypes from control mice. Colors represent different cell populations clustered by Flow Self Organizing Map (FlowSOM). (C) Mean expression of mass cytometry panel markers on each microglia subset. (D) viSNE map displaying microglia landscape from each group. (E) Ki67+ microglia (F) CD172+ microglia (G) iNOS+ microglia (H) CD38+ microglia/Total microglia percentage in each group.



## Figure 5

Minocycline treatment alleviates PTSD-like phenotype by suppressing microglial activation. (A) Microglial morphology in the HP changes upon minocycline treatment. (B) Microglia-derived inflammatory gene expression in HP after minocycline treatment, \*  $p < 0.05$  (Student t test). (C-E) Effect of minocycline on PTSD mice in fear freezing test. (F-I) Effect of minocycline on PTSD mice in open field test. (J-M) Effect of minocycline on PTSD mice in EPM test;  $n = 12$ , data are expressed as means  $\pm$  SEM, \*  $p < 0.05$ , \*\*  $p < 0.01$ , \*\*\*  $p < 0.001$  (Student's t test). (Mino: minocycline, NS: no significant)

Figure 6

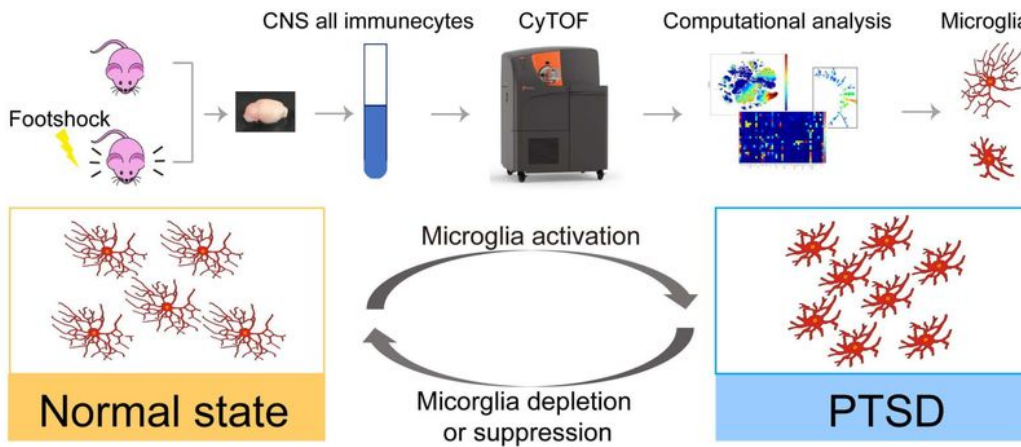


## Figure 6

Graphic abstract of microglia activation in PTSD and microglia deletion and suppression alleviates PTSD symptoms.

## Supplementary Files

This is a list of supplementary files associated with this preprint. Click to download.

- [Supplementarydata.docx](#)